A Comparison of Hydraulic and Electro-Hydraulic Power Steering Control Systems for Increasing Energy Efficiency

Meiyanto Eko Sulistyo
Department of Electrical Engineering, Universitas Sebelas Maret

Ristiana, Rina
The Research Centre for Transportation Technology, National Research and Innovation Agency, Indonesia

Kaleg, Sunarto
The Research Centre for Transportation Technology, National Research and Innovation Agency, Indonesia

Hapid, Abdul
The Research Centre for Transportation Technology, National Research and Innovation Agency, Indonesia

他

https://doi.org/10.5109/7151751

出版情報：Evergreen. 10 (3), pp.1951-1960, 2023-09. 九州大学グリーンテクノロジー研究教育センター
バージョン：

A Comparison of Hydraulic and Electro-Hydraulic Power Steering Control Systems for Increasing Energy Efficiency

Meiyanto Eko Sulistyo[1,*], Rina Ristiana[2], Sunarto Kaleg[2], Abdul Hapid[2], Sudirja[2], Aam Muharam[2], Alexander Christhanto Budiman[2], Abdul Qodir Jaelani[1], Amin[2]

[1]Department of Electrical Engineering, Universitas Sebelas Maret, Indonesia

[2]The Research Centre for Transportation Technology, National Research and Innovation Agency, Indonesia

*Corresponding Author's email: mekosulistyo@staff.uns.ac.id

(Received May 4, 2023; Revised August 15, 2023; accepted September 11, 2023).

Abstract: This research offered a comparison of hydraulic (HPS) and electro-hydraulic power steering (EHPS) hydraulic pressure characteristics. The goal is to assess the potential for energy savings if an electric motor replaces hydraulic pressure. The purpose is to calculate the potential energy efficiency if an electric motor replaces hydraulic pressure. For this comparison, HPS and EHPS were both modeled. A PI controller was developed based on these models to regulate the steering wheel position and angular motor speed. In addition, the systems are compared by using the same input reference and transient response system, and the energy consumption is computed. Thus, with the installation of an electric motor in the power steering, it has a good response, functions in an optimal region, stabilizes, and has a 59.95% increase in energy efficiency.

Keywords: Steering Wheel Position Control, Motor Speed Control, Hydraulic Power Steering, Electric Hydraulic Power Steering, PI control, Energy Efficiency.

1. Introduction

The power steering system is usually used to assist the driver in maintaining control of the steering wheel while the vehicle is turning or travelling at a low pace. It might also useful to hold while the car is traveling quickly. With the assistance of this power steering, the driver does not have to expend much effort and will not feel tired or agitated while driving, resulting in safety and comfort.

Fitts invented power steering in vehicle in 1876, and a power steering patent was issued to Robert E. Twyford of America in 1990. The advent of hydraulic power steering (HPS) technology marked the beginning of power steering technology. Fluid is used as a generating medium in HPS technology. The hydraulic pressure created by the pump and pushed by the axle through the drive belt produces high-pressure power steering oil, which is then forwarded to the steering rack and attached to both sides of the vehicle's wheels. HPS technology is simple to use but inefficient since the hydraulic pump operates even when the driver does not want power steering assistance.

EHPS (electro-hydraulic power steering) technology was also presented. EHPS technology is a complement to HPS technology in that it only operates when the driver requires assistance in adjusting or moving the steering wheel, as opposed to HPS, which operates the hydraulic pump continually. An electric motor drives a hydraulically pressured pump in EHPS technology. As the driver turns the steering wheel, an electric motor connected to it moves the front wheels of the vehicle. When the sensor detects the steering wheel's rotational direction, the steering wheel is in the correct position. EPHS is another option for reducing steering wheel movement in order to keep the steering wheel steady when the vehicle is driving at high speeds.

An energy efficiency is defined as follows: (i) energy efficiency is the optimal use of energy to achieve certain goals using specific methods in order to decrease energy consumption. In general, the optimal use of energy is based on the availability of existing energy, and energy usage becomes more efficient with the implementation of particular methods. The control methods that is applied is usually optimal control, such as optimum PID, LQR, Kalman Filter, MPC, and others. (ii) energy efficiency is the efficiency of energy use, or the ratio of energy use between the output and input of the system. A system with proper energy utilization has an efficiency close to 100%, however achieving 100% input and output is unachievable since the system contains energy losses generated by mechanical and electrical systems in a plant. Energy efficiency is attained here, as is well known, by evaluating many system designs and adding or eliminating several mechanical or electrical components to boost energy efficiency; in other words, the ratio of energy input to output grows and approaches 100%. Typically, the control methods such as PID, SMC, fuzzy logic control, feedback control, and others are used.

The following studies were conducted in order to answer the problem of energy efficiency. The HPS was adjusted

by altering the flow pressure from the air tank to push the cylinder and generate hydraulic pressure[1]. The pump pressure does not have to run continually[2]. A fundamental scientific and technical principles was used in the development of the hydraulic power steering alghorithms[3] [4] [5] [6]. The hydraulics of airflow velocity and flow control are provided in Olleh[7], Harinaldi[8], and pressure control in Amico[9]. Furthermore, the hydraulic heat pump proposed in Takata [10] and Changru [11].

Then, for heavy vehicles, EHPS technology was built in a modular manner[12] [13] [14] [15] [16]. The pump package, which includes an electronic controller, motor, pump, and reservoir, is attached to the main bracket[17] [18]. The rack and pinion gear valve has a substantial impact and is crucial in guiding the driver's actions during transitions, turning maneuvers, and low-speed driving modes. In 2019, was continued by designing an EHPS controller for smart electric buses, including a controller structure with a Luenberger observer[19] [20], sliding mode[21] and feedforward control[22]. All controllers are designed by analyzing vehicle responsibility based on the stability and controllability factors of the vehicle when the driver controls the steering wheel, taking into account uncertainty and road conditions. Thus, when the vehicle is turning and driving at moderate speeds, EHPS technology can give energy-efficient alternatives. Furthermore, the EHPS is outfitted with a control system and an observer, so the steering wheel takes on responsibility. According to Sawant[23] and Nugraha[24], an energy management system can be implemented.

According to Zang[1], Wong[3] and Nimbarte[4], energy efficiency in HPS can be attained by altering and regulating the hydraulic pressure, but energy efficiency in EHPS can be acquired by modifying and adjusting the electronic controller to indirectly regulate the motor as well as adjust the hydraulic pressure[9] [12] [13] [18]. This study, the efficiency of energy use is estimated based on the ratio of energy use between the output and input of the system. The selected system is a power steering system made up of HPS and EHPS. Assuming that the addition of an electric motor to the HPS transforms it into the EHPS and that a controller design is implemented on both of them, a system with the potential to be more energy efficient will be achieved. Some of the steps that must be taken to create an energy-efficient system are as follows: (i) built models system to understand the performance of the power steering system and to validate the system to ensure that it fits the characteristics of the real power steering system, notably HPS and EHPS. (ii) based on these two models, a PI controller is developed to regulate the steering wheel position angle on HPS and then add the motor speed angularly on EHPS using a cascade control scheme. Furthermore, the two models are compared by providing the same input reference to obtain a transient response system that is considered the identical, and then the energy consumption is calculated.

The paper is set up as follows. The power steering system is discussed in section 2. Section 3 contains a presentation of the PI control design. The simulation and debate are detailed in section 4, while section 5 of the report presents study conclusions.

2. Power Steering System

This section's modeling method makes use of time domains. The time domain modeling technique is designed to understand the system's features and evaluate the system in order to establish a match between the model and the actual system. This study covers two types of power steering as follows:

2.1 Hydraulic Power Steering

The HPS model is provided as a linear model that represents a dynamic system and analyzes its robustness and stability. The motion of the steering rack is translated into linear motion, which comprises all of the system's motion. The hydraulic system is activated by a difference in the steering wheel angle and the rack position. This variation is caused by the displacement of the valve, which controls the pressure in the hydraulic cylinder. The HPS components seen in Fig. 1 are the steering wheel, steering column, rack, and pinion. Based on Fig. 1, the following mathematical equations illustrate the interaction connection between HPS components[25] [26] [27] [28] [29]. The steering wheel's force is detailed below:

$$J_w\ddot{\theta}_w(t) + b_w\dot{\theta}_w(t) + k_w\big(\theta_w(t) - x_r(t)\big) = \frac{1}{r_r}T_d(t) \quad (1)$$

with J_w is the steering wheel's moment of inertia, θ_w is the angle of the steering wheel, b_w is the steering wheel's viscous damping, k_w is the spring coefficient of the torsion bar, x_r is the rack position, r_r is the gear radius of the pinion, and T_d is the steering wheel torque. The rack's force, including the tires, equals

$$M_r\ddot{x}_r(t) + b_r\dot{x}_r(t) + k_w\big(x_r(t) - \theta_w(t)\big) - \rho_L A_p(t) + F_l(t) = 0 \quad (2)$$

with M_r, b_r, A_p, ρ_L, and F_l denoting the rack mass, rack damping coefficient, cylinder area, oil density, and external load acting on the steering rack, respectively. The hydraulic system is described as follows:

$$\dot{\rho}_L(t) = -\frac{k_c}{C_h}\rho_L(t) + \frac{k_q}{C_h}x_v(t) - \frac{A_p}{C_h}\dot{x}_r \quad (3)$$

with k_c is the linearized flow-pressure coefficient, k_q is the flow gain, and C_h is the hydraulic capacitance. The difference in the steering wheel and rack position causes the valve to open where is $x_v(t) = \theta_w(t) - x_r(t)$.

A state space model of the open loop system is used in the linear analysis of the system's stability margins. The

majority of the elements in the model are connected to the mechanical of the structure, such as masses, spring coefficients, and viscous damping; moreover, hydraulic coefficients that change depending on the working points are included. In order to undertake the margin analysis of the system's stability, the working point dependency of the hydraulic coefficient must be defined. The HPS linear system may be expressed in state space form as follows:

$$\dot{x}_h(t) = A_h x_h(t) + B_h u_h(t) + H_h d_{Lh}$$
$$y_h(t) = C_h x_h(t) \quad (4)$$

with $A_h \in R^{n\times n}$, $B_h \in R^{n\times m}$, $C_h \in R^{m\times n}$, $x_h(t) \in R^n$, and $u_h(t) \in R^m$.

Based on (1) to (3), The state variable defined: $x_h(t) = [\theta_w(t) \quad \dot{\theta}_w(t) \quad x_r(t) \quad \dot{x}_r(t) \quad \rho_L(t)]^T$, with $\theta_w(t) = x_{h1}(t)$, $\dot{\theta}_w(t) = x_{h2}(t)$, $x_r(t) = x_{h3}(t)$, $\dot{x}_r(t) = x_{h4}(t)$, and $\rho_L(t) = x_{h5}(t)$. The input variable defined $u_h(t) = T_d(t)$, and the output variable is $\theta_w(t)$. The matrices of A_h, B_h, and C_h on (4) are describes as

$$A_h = \begin{bmatrix} 0 & 1 & 0 & 0 & 0 \\ \frac{-k_w}{J_w} & \frac{-b_w}{J_w} & \frac{k_w}{J_w} & 0 & 0 \\ 0 & 0 & 0 & 1 & 0 \\ \frac{k_w}{M_r} & 0 & \frac{-k_w}{M_r} & \frac{-b_r}{M_r} & \frac{A_p}{M_r} \\ 0 & 0 & 0 & \frac{-A_p}{C_h} & \frac{-k_c}{C_h} \end{bmatrix},$$

$$B_h = \begin{bmatrix} 0 & \frac{1}{J_w r_r} & 0 & 0 & 0 \end{bmatrix}^T,$$

$C_h = [1 \quad 0 \quad 0 \quad 0 \quad 0]$, $H_h = [0 \quad 0 \quad 0 \quad 1 \quad 1]^T$, and

$$d_{Lh} = \begin{bmatrix} 0 & 0 & 0 & -F_l & \frac{k_q}{C_h} \end{bmatrix}$$

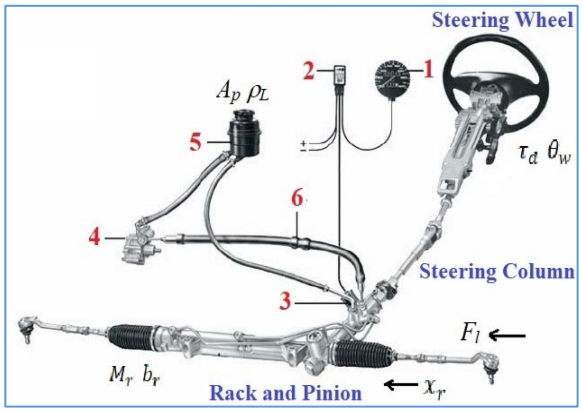

(1) Electronic speedometer, (2) ECU, (3) Electrohydraulic transducer, (4) Engine driven pump, (5) Oil reservoir, (6) Hose pipe

Fig. 1: HPS System

2.2 Electro-Hydraulic Power Steering (EHPS)

The EHPS model is nearly identical to the HPS model, the only difference being that there is an addition of an electric motor to the pump, as illustrated in Fig. 2. The steering wheel force and hydraulic system in the EHPS model are the same as in equations (1) and (3). The installation of the electric motor system that characterizes the EHPS system, or the equation's electric motor, is as follows:[26) 30)]

$$V_m(t) = L_m \dot{i}_m(t) + R_m i_m(t) + k_e \dot{\theta}_m(t) \quad (5)$$
$$J_m \ddot{\theta}_m(t) + b_m \dot{\theta}_m(t) - k_t i_m(t) = T_m(t) - T_l(t) \quad (6)$$

with V_m, L_m, i_m, and k_e denoting the motor voltage, mutual inductance, motor current, and the back emf constant, respectively. Moreover, $\dot{\theta}_m$, J_m, b_m, θ_m, and T_m are the speed, inertia moment, damping coefficient, position angle, and torque of the motor, respectively. Because there is an addition of an electric motor, equations (2) and (6) are substituted as follows:[25) 26) 27) 28)]

$$J_{eq}\ddot{\theta}_m(t) + b_{eq}\dot{\theta}_r(t) + N_r{}^2(k_w + k_s)\theta_m(t) -$$
$$k_w\theta_w(t) - \rho_L A_p(t) + F_l(t) - T_m = 0 \quad (7)$$

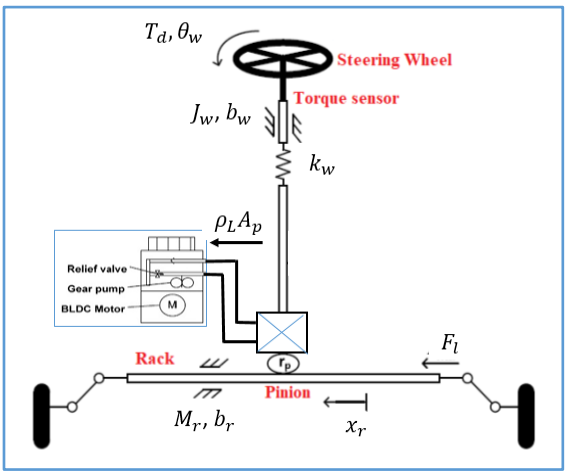

Fig. 2: EHPS System

The EHPS linear system may be expressed in state space form as follows:

$$\dot{x}_{eh}(t) = A_{eh}x_{eh}(t) + B_{eh}u_{eh}(t) + H_{eh}d_{Leh}$$
$$y_{eh}(t) = C_{eh}x_{eh}(t) \quad (8)$$

with $A_{eh} \in R^{n\times n}$, $B_{eh} \in R^{n\times m}$, $C_{eh} \in R^{m\times n}$, $x_{eh}(t) \in R^n$, and $u_{eh}(t) \in R^m$. Based on (1), (7), (3), and (5), The specified state variable $x_{eh}(t) = [\theta_w(t) \ \dot{\theta}_w(t) \ i_m(t) \ \theta_m(t) \ \dot{\theta}_m(t) \ \rho_L(t)]^T$, with $\theta_w(t) = x_1(t)$, $\dot{\theta}_w(t) = x_2(t)$, $i_m(t) = x_3(t)$, $\theta_m(t) = x_4(t)$, $\dot{\theta}_m(t) = x_5(t)$, and $\rho_L(t) = x_6(t)$. Specified by the input variable $u_{eh}(t) = [T_d(t) \quad V_m(t)]$, and the output variable is $\theta_w(t)$ and $\dot{\theta}_m(t)$. The matrices of A_{eh}, B_{eh}, and C_{eh} on (7) for (1) to (6) are describes as:

$$A_{eh} = \begin{bmatrix} 0 & 1 & 0 & 0 & 0 & 0 \\ \frac{-k_w}{J_w} & \frac{-b_w}{J_w} & 0 & \frac{k_w}{J_w} & 0 & 0 \\ 0 & 0 & \frac{-R_m}{L_m} & 0 & \frac{-k_e}{L_m} & 0 \\ 0 & 0 & 0 & 0 & 1 & 0 \\ \frac{k_w}{J_{eq}} & 0 & 0 & \frac{-N_r{}^2(k_w+k_s)}{J_{eq}} & \frac{-b_{eq}}{J_{eq}} & \frac{A_p}{J_{eq}} \\ 0 & 0 & 0 & 0 & \frac{-A_p}{C_h} & \frac{-k_c}{C_h} \end{bmatrix},$$

$$B = \begin{bmatrix} 0 & \frac{1}{J_w r_r} & 0 & 0 & \frac{1}{J_{eq} L_m} & 0 \end{bmatrix}^T,$$

$$C = [1 \quad 0 \quad 0 \quad 0 \quad 1 \quad 0],$$
$$H = [0 \quad 0 \quad 0 \quad 0 \quad 1 \quad 1]^T, \text{ and}$$

$$d_L = \begin{bmatrix} 0 & 0 & 0 & 0 & -F_l & \frac{k_q}{C_h} \end{bmatrix}.$$

3. The PI Controller Design

In this section describes the controller design to be applied in HPS and EHPS systems. The controller design using PI controller. The PI controller is a classic control but it is extensively utilized, easy to locate in physical form, and simple to create or modify to apply, particularly in power steering systems. Thus, the usage of PI control and its design become fascinating topics, particularly in PI control tuning, where several research has been ongoing.

In this study, the controller was built in two modes. First, the PI controller on the HPS system is utilized to regulate the steering wheel position angle $\theta_w(t)$ in its implementation, as illustrated in Fig. 3a. Last, the cascade control approach is used to set the motor speed angle $\dot{\theta}_m(t)$ and steering wheel position angle $\theta_w(t)$using the PI controller, as shown in Fig. 3b.

The proportional (P) and integral (I) controllers make up the PI controller. By tuning the K_p and K_i gains, the PI controller is designed. The goal of this tuning is to produce a system with a satisfactory output response that has a steady-state error and reaches a proper steady-state and transient time. The following equation describes the PI controller;[25) 30) 31) 32)]

$$u_c(t) = K_p e(t) + K_i \int_0^t e(\tau)\ d\tau \tag{9}$$

with $e(t)$ is the error state determined from difference the desired output system $\theta_w(t)$ or $\dot{\theta}_m(t)$ with the input reference $\theta_{w,ref}(t)$ or $\dot{\theta}_{m,ref}(t)$, can be written;

$$e_w(t) = \theta_{w,ref}(t) - \theta_w(t)$$
$$e_m(t) = \dot{\theta}_{m,ref}(t) - \dot{\theta}_m(t) \tag{10}$$

The PI controller is written in the form of a transfer function

$$G_c(s) = \frac{U_c(s)}{E_\theta(s)} = \frac{1}{\left(1+\frac{K_i}{s}\right)K_p} \tag{11}$$

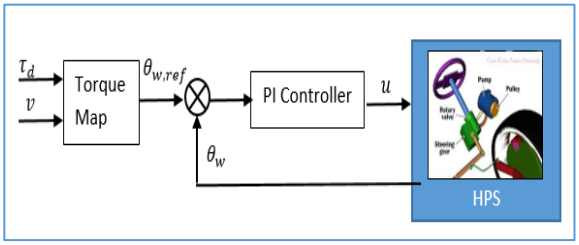

a) PI Controller of HPS

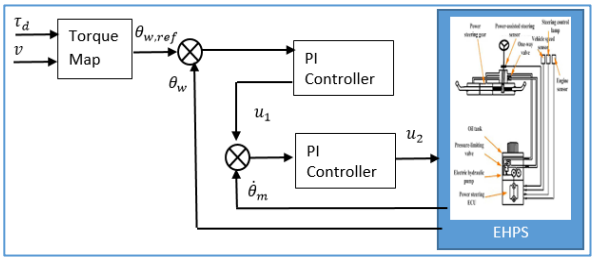

b) PI Controller of EHPS

Fig. 3: PI Controller Design

The transfer function for equations (4) and (8) is written as follows:

$$G_s(s) = \frac{Y_v(s)}{U_c(s)} = [C_v(sI - A_v)^{-1}B_v] \tag{12}$$

Terms: $G_s(s)$ is a system of order-2 as follows $G_s(s) = s^2 + as + b$. For a multi-order system, it can be obtained to be a 2-order system by selecting two dominant poles that represent the system. The close-loop system can be illustrated as shown in the block diagram of Fig. 4. For example, a closed system from $\theta_{w,ref}(s)$ to $\theta_w(s)$ is obtained:

$$\frac{\theta_w(s)}{\theta_{w,ref}(s)} = \frac{K_p(s+K_i)}{s^2+(a+K_p)s+bK_pK_i} \tag{13}$$

To get the transient response of the second-order system, the K_p and K_i gains are tuned using the characteristic equation of the second-order system. The following may be used to write the characteristic equation:

$$s^2 + 2\zeta\omega_n s + \omega_n = 0 \tag{14}$$

where ζ is the damping ratio and ω_n is the damping factor. ζ to determine the deviation, while ω_n to determine the settling time and steady time. To obtain the transient response of a 2nd-order system, the denominator of the 2nd-order system is the same as the 2nd-order characteristic equation, written as follows;

$$s^2 + (a + K_p)s + bK_pK_i = s^2 + 2\zeta\omega_n s + \omega_n{}^2 \tag{15}$$

Thus it can be determined the value of $K_p = 2\zeta\omega_n - a$, and $K_i = {\omega_n{}^2}/{bK_p}$.

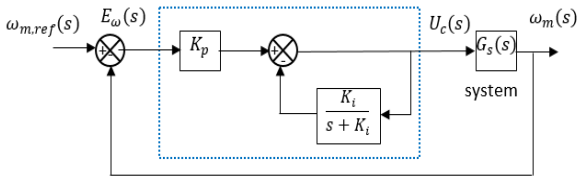

Fig. 4: Block Diagram PI Controller

4. Simulation and Discussion

This section discusses about the validation system by conducting simulations in order to obtain a fit of the model built with the real of the power steering system. The validation of the performance system includes model analysis for each subsystem (including hydraulic, electric motor, and torque map characteristics) and open-loop system analysis based on system transient response. Then apply the PI controller design to the power steering system. Next, do an analysis stability system to get the tolerance of the resistance system. Furthermore, both models are compared by providing the same input reference to obtain a transient response system that is considered the same, then the energy consumption is calculated. Then the validate system by conducting simulations in order to obtain a match between the model built and the real power steering system, including; hydraulic characteristics, determining the torque map, analyzing the transient response system, and calculating energy consumption to achieve the most efficient power steering system. Finally, compared the performance of HPS systems with EHPS to get energy efficiency.

Table 1. The Parameters of HPS and EHPS

Symbol	Parameter	Value	Unit
J_w	Moment inertia of steering wheel	0.0258	Kgm^2
b_w	Damping coefficient of steering wheel	0.742	Nm s/rad
k_w	Torsional stiffness of torque sensor	2.5	Nm/rad
r_r	Gear radius	0.05	m
M_r	Rack mass	32	Kg
b_r	Damping coefficient of rack	35283	Nm s/rad
b_c	Lateral viscous damping of steering column	1.53	Nm s/rad
k_s	Lateral spring coefficient of the tire	2.5	Nm/rad
F_{load}	External load acting on the steering rack	0.027	Nm
A_v	Cylinder area	0.00925	m^2
C_h	Capacitance hydraulic	1.75	cc/rev
R_m	EHPS motor resistance	0.007	Ohm
L_m	EHPS motor inductance	5.1x10^{-4}	H
J_m	Inertia moment of the EHPS motor	1.38x10^{-6}	Kgm^2
b_m	Damping coefficient of the EHPS motor	6.8x10^{-5}	Nm s/rad
k_e	Back-emf constant of the EHPS motor	0.0585	V.s/rad
k_t	Torque constant of the EHPS motor	0.0495	Nm s/rad
N_r	Gear ratio	13.65	

Fig. 5: BRIN Minibus

For simulation needs, the HPS model (4) and the EHPS model (8) are included in some of the parameters provided in Table 1 thought numerical parameterization. Some of the parameters listed in Table 1 are obtained from the component datasheet, and for some parameter values that were needed but not found on the datasheet, identification was carried out by measuring directly to the real power steering system on BRIN minibuses, as shown in Fig. 5, which also calculates some of the necessary parameters based on the general formula of physics. These parameters correspond to the real condition of the actual installed HPS and EHPS on minibus vehicles.

4.1 Hydraulic Characteristics

The valve hydraulic characteristic is depicted in Fig. 6a, where the valve area openings are represented as a function of steering wheel torque applied. As the valve displacement is directly proportional to a generated load pressure, the typical power steering is based on a valve controlled (open center - A1) and a pump flow controlled (close center - A2). In actuality, the enlarged area is restricted by the valve and the level off ranges from 20 to 30 mm2. The value still in the tolerance of the performance system. The connection between the load pressure and the steering wheel torque produced by the hydraulic system is seen in Fig. 6b. When the steering rack velocity is low, the curve is only applicable. The resultant load pressure is also quasi statically impacted by the load flow, which is caused by rack motion. Depending on the motion's direction, the pressure will rise or fall.

The displacement pump is a fixed directly driven electric pump and a flow control valve. The pump is chosen mostly based on the system's energy consumption. Figures 6c and 6d illustrate how the pump's typical flow pressure fluctuates with temperature and pressure. Figures 6c and 6d show the power steering pump's flow pressure characteristics as a function of temperature fluctuation and pump speed at 850 and 1500 revolutions per minute, respectively. The dominated characteristic is the pump speed at 1500 rpm whereas the characteristic of the flow controller is noticeable.

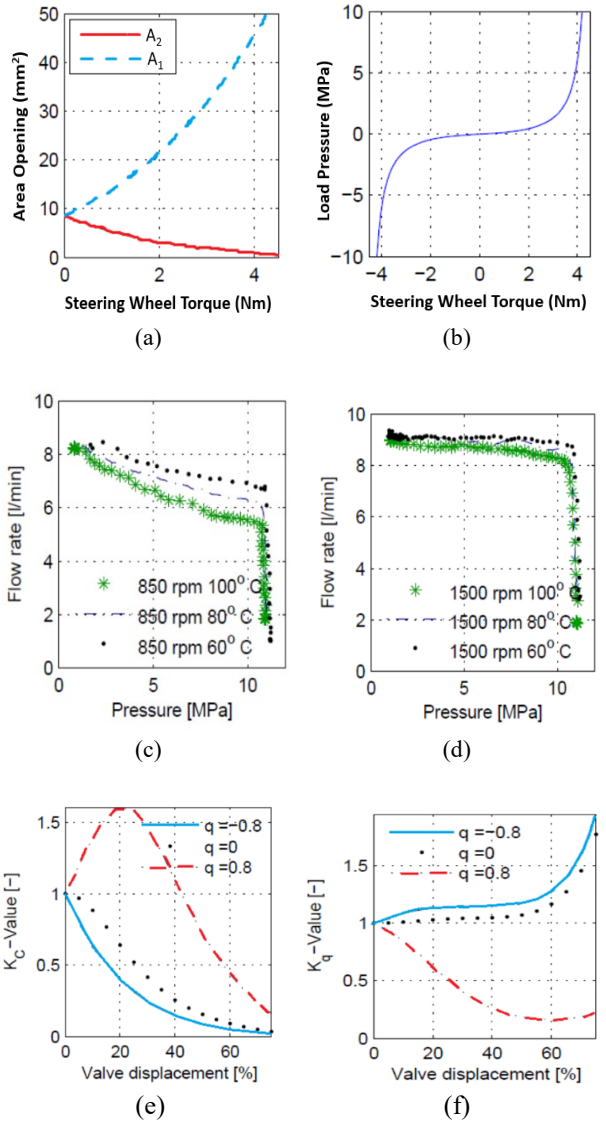

Fig. 6: The Characteristics Responses of the Hydraulic System

The hydraulic coefficient in (3), there are the linearized flow-pressure coefficient (k_c) and the flow gain (k_q). Both coefficients must be calculated in order to analyze the stability of the power steering system and to calculate the system's margin stability. The actual valve displacement and load flow affect both coefficients. As can be seen in Fig. 6e for the linearized flow-pressure coefficient and Fig. 6f for the flow gain, the load flow is normalized in relation to the system flow and the load flow (q).

4.2 Torque Map

The torque map is then determined by identifying the response system and supplying a load torque value and a torque map under zero circumstances ($\tau_l = 0, h = 0$). The power steering system's characteristics were determined using data acquired on the assist motor current (i_m) from the current sensor and the driver torque (τ_d) from the torque sensor. Figure 7 depicts the relationship between assist motor current (i_m) and steering driver torque (τ_d) at three different vehicle speeds: 0 km/h, 40 km/h, and more than 240 km/h. To obtain the assist value for motor torque (τ_a), multiply the motor torque constant by two.

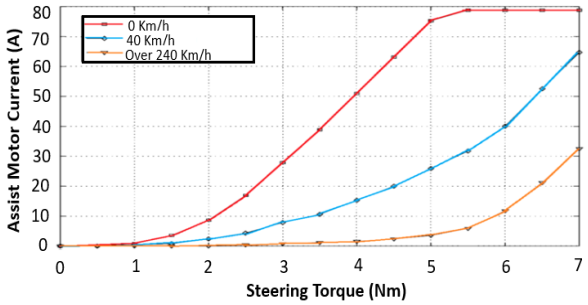

Fig. 7: Torque Map Characteristics

4.3 The Response Transient System

The next step is to look at the response transient system, which is the correlation between the motor speed, velocity flow, flow control valve, and pump flow control. As an ideal reference, a hydraulic-based power steering refers to the hydraulic characteristics and for the input system pattern using a torque map which explains the relationship between motor current and steering torque to vehicle speed.

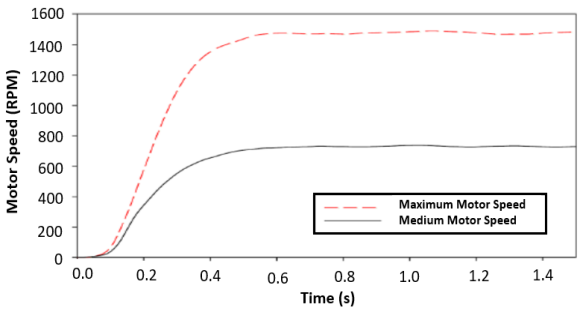

(a) Electric Motor

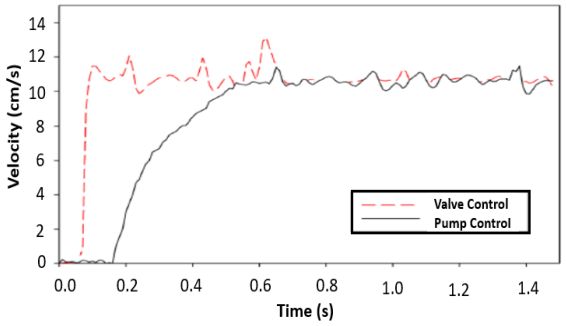

(b) Hydraulic

Fig. 8: Response Transient System

For the valve flow control system, the motor speed was maintained at 1450 rpm, and it was changed from 0 to 1450 rpm in accordance with the control scheme for the pump flow control system as illustrated in Fig. 8a. The comparison of velocity response of valve and pump flow shows in Fig. 8b. Pump flow control responded more

quickly than valve flow control. The delay time, rise time, and settling time for the valve flow control are 0.05, 0.01, and 0.01 seconds, respectively, while the delay time for the pump flow control is 0.14, 0.28, and 0.45 seconds, respectively. This means the maximum motor speed is set at 1450 rpm and for the motor speed rate at 700 rpm which has the delay time, rise time, and settling time about 0.14, 0.28, and 0.45 seconds, respectively. It can see that the response motor speed is proportional with the pump flow. At maximum motor speed, velocity of valve control and velocity of pump control both reach an average of 10 cm/s, the difference is the delay time and rise time for both. Thus it can be obtained the relationship of response characteristics between the electric motor and the hydraulic part.

Referred to the power steering characteristics, the next step is to compare the performance of the HPS and EHPS systems based on the models in equations (4), (8), and Table 1. The response system for the open-loop can be seen in Fig. 9 and Fig. 10. The HPS and EHPS systems are given the same input response ($T_d(t)$) as shown in Fig. 3 and a different response can be seen for the flow pressure pump. In Fig. 9, HPS only has a hydraulic drive, so a velocity response system can be obtained between the pump (black line) and valve control (red line). Based on the velocity response system, the steering wheel angle (blue line) value is obtained but this value does not reach the desired reference value (dash-black line). The HPS performance

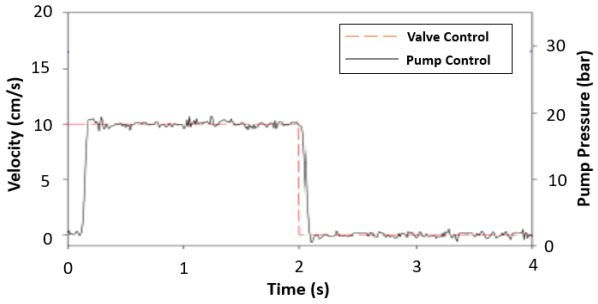

(a) Hydraulic Response

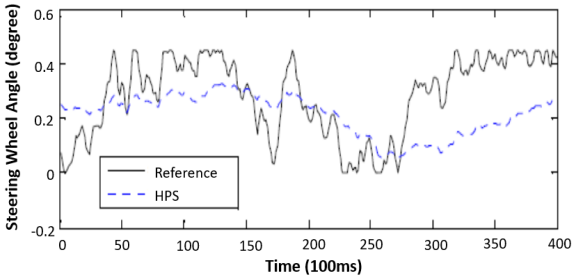

(b) Output Response

Fig. 9: Open Loop System of HPS

has a transient response that cannot reach the specified reference value (Fig. 9b) and the energy used to reach the reference is calculated, the HPS with a pressure of 20 bar and a velocity of 10 cm/s (Fig. 9a) used approximately 2758 watt-hours.

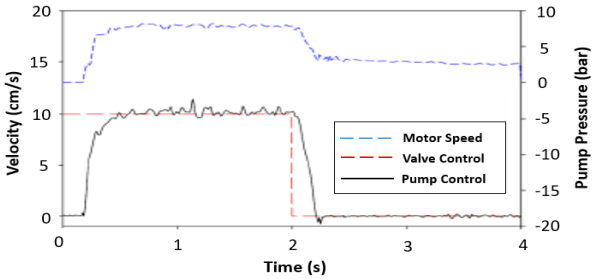

(a) Hydraulic and Motor Electric Response

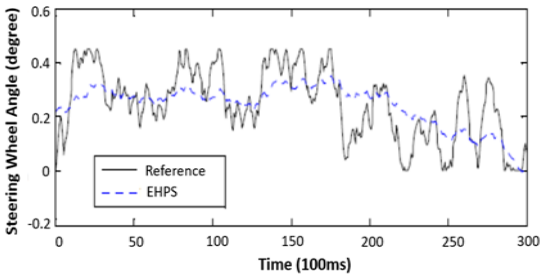

(a) Output Response

Fig. 10: Open Loop System of EHPS

In Fig. 10, an electric motor drives the hydraulic system, allowing the velocity response system to be obtained at the left side between the pump (black line), valve control (red line), and motor speed (blue line). Based on the velocity response system, the steering wheel angle value (blue line in right-side) is obtained and a smooth response is obtained and achieves the desired reference value (dash-black line in right-side). The EHPS transient response can achieve the specified reference value but it still has a big oscillation (Fig. 10b) while the EHPS with a pressure of 5 bar, a velocity of 10 cm/s, and a motor speed of 700 rpm (Fig. 10a) used approximately 400 watt-hours. As a result, adding an electric motor to an EHPS can lower energy consumption by 58.95%.

The PI controller gains were empirically modified using the second-order characteristic equation approach, as described in (15). The controller gains of the steering wheel angle was found to be $K_p = 0.01$, and $K_i = 0.0001$. Controller gains of the motor speed was found to be $K_p = 0.02$, and $K_i = 0.00025$. The closed-loop system, specifically for EHPS, enhanced the tracking capabilities of the hydraulic velocity control (including pump flow, valve flow, and pressure pump), steering wheel angle, and motor speed. The transient response closed-loop is depicted in Fig. 11. By adding a PI controller, both HPS (blue-line in left-side) and EHPS (blue-line in right-side) can achieve the desired reference value. Thus, based on the same input reference to obtain a transient response system that is considered the same, then the energy consumption is calculated. The performance of the closed-loop system (system with controller) may be

shown in Fig. 11. Both HPS and EHPS can reach the system's reference and make the system more responsive.

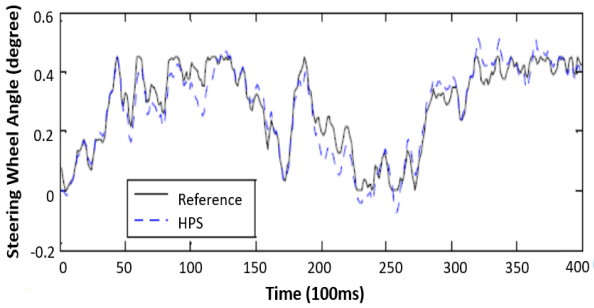

(d) HPS

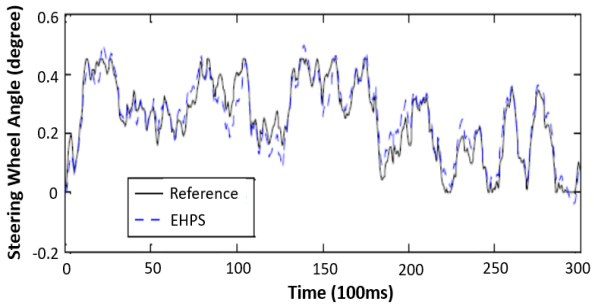

(e) EHPS

Fig. 11: Close Loop System of HPS

The energy consumption shows in Fig. 12. The same trends could be observed as the HPS and EHPS. Energy consumption is calculated based on several parts of the mechanical and electric system or namely the engine. In HPS there are belt drive, pump, and gear box hydraulic sections, while in EHPS there are generators, electric motors, power network, gear box of motors and steering. In addition, energy consumption is also calculated based on the vehicle at idle and traveling at low speed (40 Km/h) as shown in Fig. 7. Similarly, for energy consumption, Fig. 12a shows that with a 30 bar pressure pump, the average energy use is 2200 watt-hours, but in EHPS, Fig. 12b shows that with a pressure pump rate of 16 bar, the average energy use is 170 watt-hours. The energy efficiency of the system before and after the controller is implemented may be observed in the comparison. Energy may be lowered by approximately 25.36% for HPS and around 57.5% for EHPS. As a result, the comparison of energy ratios may be stated as follows: (i) for HPS, the difference between HPS benchmark (without controller) and HPS with controller is 25.36%. (ii) the ratio of EHPS benchmark (without controller) to EHPS with controller is 57.5%. (iii) when comparing the usage of HPS and EHPS, the energy use ratio is roughly 58.95%, indicating that EHPS is more energy efficient than HPS.

Based on the direct measure on minibus, the average energy consumptions of HPS is 2328.07 watt-hours and EHPS is 132.48 watt-hours. Table 2 provides an overview of the performance attained in HPS and EHPS. According to the simulation results, HPS has an energy efficiency of 22% with a power loss of around 70 watt-hours, whereas EHPS has an energy efficiency of 60% with a power loss of approximately 30 watt-hours. Thus the EHPS technology with the addition of an electric motor as a pump driver makes the power steering more energy efficiency and reduce energy consumption. Thus, the discrepancy between simulation and measurement findings is 0.105%, indicating that the system validation results are valid.

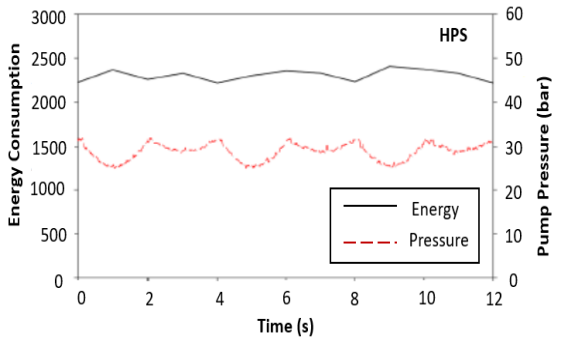

(a) HPS

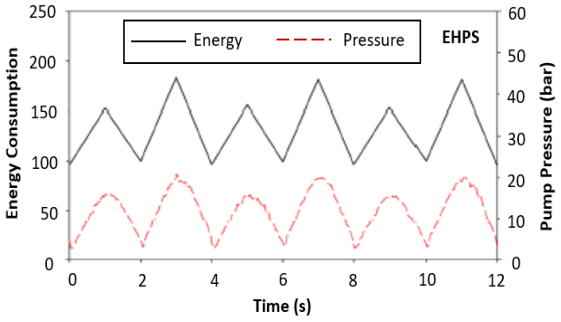

(b) EHPS

Fig. 12: Energy Consumption

Table 2. The Energy Consumption

Hydraulic			Electro-Hydraulic		
Engine	**Energy Consumption**		**Engine**	**Energy Consumption**	
	Idle	**Driving**		**Idle**	**Driving**
Belt Drive	0.95	10	Generator	0.45	10
Pump	0.7	40	Power Network	0.85	10
Gear Box Hydraulic	0.9	20	Electric Motor	0.7	20
			Gear Box Motor	0.85	0
			Gear Box Steering	0.95	0
Efficiency	40%		Efficiency	88%	
Power Loss	70 W		Power Loss	30 W	

5. Conclusions

The comparison of the hydraulic pressure characteristics of HPS and EHPS to control the steering wheel position has been proposed. The hydraulic pressure has an important role to move the steering wheel position and get energy-efficient consumption. An efficiency

energy of the HPS can be obtained by modifying and adjusting the hydraulic pressure, while in the EHPS, efficiency energy can be carried out on the electronic controller to regulate the motor indirectly as well as adjust the hydraulic pressure. For the purposes of this comparison, HPS and EHPS modeling were carried out using the time domain approaches. The use of both models, a PI controller is designed constructed to regulate the steering wheel's position angle on the HPS and for EHPS added to control the angular motor speed with the cascade control scheme. Both PI controller designs are compared by providing the same input map torque reference to see the power steering performance and calculated the energy consumption.

The simulation results show, the comparison of energy ratios may be stated as follows: (i) for HPS, the difference between HPS benchmark (without controller) and HPS with controller is 25.36%. (ii) the ratio of EHPS benchmark (without controller) to EHPS with controller is 57.5%. (iii) when comparing the usage of HPS and EHPS, the energy use ratio is roughly 58.95%, indicating that EHPS is more energy efficient than HPS. Thus, with the addition of an electric motor in the power steering, it has the same hydraulic pressure characteristics but has more energy-efficient. The relationship between the hydraulic pressure characteristics with the steering wheel position of the hydraulic-based power steering can be used to design hydraulic-based active power steering for future work, and further control strategies can be developed such as robust control for steering system stability, optimal control for optimizing steering wheel torque and pressure hydraulic, and intelligent control for active power steering.

Acknowledgements

This work is supported by The National Research and Innovation Agency (BRIN) of Indonesia and uses the research budget at the program house of electric vehicle technology. Rina Ristiana, Sunarto Kaleg, and Sudirja are the main contributors of this paper. All authors read and approved the final paper. The authors do not have any type of conflict of interest to declare.

References

1) Z. Yang, R. Wang, L. Zhang, C. Yu, G. Shi and H. Chen, "A New Hydraulic Power Steering System for Hydrib City Bus," Vols. 321-324, 2013
2) K. Zheng, T. Shen, Y. Yau, J. Kako, S. Yosida, “Load Torque Analysis Based on The Integrated Model of HPAS Systems”, Vehicle Power and Propulsion Conference, 2008.
3) T. Wong, "Hydraulic Power Steering System Design and Optimization Simulation," in *Steering and Suspension Technology Symposium* , Detroit, Michigan, 2001
4) M. R. Nimbarte and L. Raut, "Efficiency Analysis of Hydraulic Power Steering System," *International Journal of Engineering Research and Applications,* vol. 3, no. 3, pp. 1230-1235, 2013
5) W. Liu, R. He, Z. You, “ Analysis of Assist Characteristic of Electric Hydraulic Power Sreeting System”, Computer Modelling and New Technologies, vol. 18, No. 12D, pp.46-50, 2014.
6) T. Ensbury, P. Harman, M. Demsey, “Modelling and Development of a Pseudo-Hydraulic Power Steering Model for Use in Real-Time Applications”, The 2nd Japanese Modelica Conference Tokyo, Japan, 2018.
7) N. Olleh, N. Husain, H. Kamar, N. Kamsah and M. I. Alhamid, "Outlets Airflow Velocity Enhancement of an Automotive HVAC Duct," *EVERGREEN Joint Journal of Novel Carbon Resource Sciences & Green Asia Strategy,* vol. 8(1) 163-169 (2021). https://doi.org/10.5109/4372273
8) Harinaldi, M. D. Kesuma, R. Irwansyah, J. Julian and A. Satyadharma, "Flow Control with Multi-DBD Plasma Actuator on a Delta Wing," *EVERGREEN Joint Journal of Novel Carbon Resource Sciences & Green Asia Strategy,* vol. 7(4) 602-608 (2020). https://doi.org/10.5109/4150513
9) Alessandro Dell’Amico, “*On Electrohydraulic Pressure Control for Power Steering Applications Active Steering for Road Vehicle*”, Dissertation Division of Flui and Mechatronic System Department of Management and Engineering Linkoping University, 2016
10) J. Ko1, N. Takata, K. Thu and T. Miyazaki, "Dynamic Modeling and Validation of a Carbon Dioxide Heat Pump System," *EVERGREEN Joint Journal of Novel Carbon Resource Sciences & Green Asia Strategy,* vol. 7(2) 172-194 (2020). https://doi.org/10.5109/4055215
11) Y. Changru, N. Takata, K. Thu and T. Miyazaki, "How Lubricant Plays a Role in the Heat Pump System," *EVERGREEN Joint Journal of Novel Carbon Resource Sciences & Green Asia Strategy,* vol. 8(1) 198-203 (2021). https://doi.org/10.5109/4372279
12) J. E. Forbes, S. M. Baird and T. W. Weisgerber, "Electrohydroulic Power Steering - An Advanced System for Uniquie Applications," vol. 96, no. 2, 1987.
13) L. Xia, and H. Jiang, “An Electronically Controlled Hydraulic Power Steering System for Heavy Vehicle”, Advanced in Mechanical Engineering, vol 8, issue 11, 2016.
14) J. Loof, I. Besselink, W. Post, H. Nijmeijer, “Development of A Truck Steering System Model Including Hydraulics to Predict the Steering Wheel Torque’, International Conference Graz Sysposium Virtual Vehicle, 2016.
15) J. Loop, I. Besselink, H. Nijmeijer, “Full Scale Truck Steering System Modelling and Validation”, International Conference AVEC 2016.

16) J. Song, L. Lu, W. Xuan, L. Yu, “Electro-hydraulic Power Steering System for Commercial Vehicles”, Journal of Tsinghua University. vol. 54. No. 9, pp.1209-1214, 2014.
17) V. Jaiganesh, “Incorporation of Both Inner and Counter Face Mechanism in a Vehicle with The Help of Electro Hydraulic Systems”, International Conference on Advances in Design and Manufacturing (ICAD&M), 2014.
18) H. Du, Q. Zhang, S. Chen, Modeling, Simulation, and Experimental Validation of Electro-Hydraulic Power Steering System in Multi-Axle Vehicles”, Journal of Automobile Engineering, vol. 233, No. 2, 2017
19) A. Li, W. Yuan, S. Li, X. Wang, X. Qiu and L. Xu, "Design and Implementation of Controller for EHPS of Intelligent Electric Bus," vol. 7, 2019
20) R. Ingenbleek, X. Yin, H. Schwarz, “Observer Canonical Forms for Biliniear Systems and an Application to Translatory Hydraulic Drives via Parameter Identification”, International Journal System Anlysis Modelling Simulation, 1993.
21) P. Bachman, “Using Sliding Mode Control in Control of Electro Hydraulic Servo Drive”, in e-book: A Hydraulika and Pneumatika, Hydrocom, Rocnik VIII, edition 3-4, 2006.
22) F. Momiyama, E. Kitagishi and T. Noriaki, "Electro-Hydraulic Feedforward Control Power Steering System for Trucks and Busses," 1989.
23) S. Sawant, R. M. R. A. Shah, M. Rahman, A. R. A. Aziz, S. Smith and A. Jumahat, "System Modelling of an Electric Two-Wheeled Vehicle for Energy Management Optimization Study," *EVERGREEN Joint Journal of Novel Carbon Resource Sciences & Green Asia Strategy,* vol. 8(3) 642-650 (2021). https://doi.org/10.5109/4491656
24) G. D. Nugraha, B. Sudiarto and K. Ramli, "Machine Learning-based Energy Management System for Prosumer," *EVERGREEN Joint Journal of Novel Carbon Resource Sciences & Green Asia Strategy,* vol. 7(2) 309-313 (2020). https://doi.org/10.5109/4055238
25) R. Walters, Hydraulic and Electro-Hydraulic Control System, Springer, 2000.
26) R. L. Woods, K. L. Lawrence, “Modeling and Simulation of Dynamic Systems”, Prentice Hall, 1997.
27) A. Zhuan, H. Ren, L. Renhe, L. Qiongqiong, “Electric Hydraulic Power Steering System Design Based on Electric Motor Coach of Mixed H2/H∞ Control”, International Journal of Control and Automation, vol. 9, No. 7, pp.263-272, 2016.
28) R. Ristiana, S. Kaleg, R. Mardiati, A. Muharam, A. Hapid, A. C. Budiman, K. Ismail, “Wireless Position Control of an Electric Power Steering System for Energy Optimization”, 16th International Conference on Telecommunication Systems, Services, and Applications (TSSA), 2022.
29) A. Cui, S. Wang, Y. Qu, X. Chen, “Parameters optimization of electro-hydraulic power steering system based on multi-objective collaborative method”, Generalized Dynamics Modeling and Dynamics Control of Autonomous Driving Vehicle, 2023.
30) R. Ristiana, A. Syaichu-Rohman, C. Machbub, A. Purwadi and E. Rijanto, "A New Approach of EV Modeling and its Control Application to Reduce Energy Consumption," *IEEE Access,* vol. 7, pp. 141209-141225, 2019.
31) H. Ibrahim, F. Hassan and A. Shomer, "Optimal PID Control of a Brushless DC Motor using PSO and BF Techniques," *Ain Shams Engineering Journal,* vol. 5, 2014.
32) P. Antsaklis and Z. Gao, Control Systems Design, McGraw-Hill, 2005.